



HAL
open science

Quantitative monitoring of dissolved gases in a flooded borehole: calibration of the analytical tools

Van-Hoan Le, Marie-Camille Caumon, Jacques Pironon, Philippe de Donato, Médéric Piedevache, Aurélien Randi, Catherine Lorgeoux, Odile Barres

► To cite this version:

Van-Hoan Le, Marie-Camille Caumon, Jacques Pironon, Philippe de Donato, Médéric Piedevache, et al.. Quantitative monitoring of dissolved gases in a flooded borehole: calibration of the analytical tools. 16th International Conference on Greenhouse Gas Control Technologies, Oct 2022, Lyon, France. hal-03879151

HAL Id: hal-03879151

<https://hal.science/hal-03879151v1>

Submitted on 30 Nov 2022

HAL is a multi-disciplinary open access archive for the deposit and dissemination of scientific research documents, whether they are published or not. The documents may come from teaching and research institutions in France or abroad, or from public or private research centers.

L'archive ouverte pluridisciplinaire **HAL**, est destinée au dépôt et à la diffusion de documents scientifiques de niveau recherche, publiés ou non, émanant des établissements d'enseignement et de recherche français ou étrangers, des laboratoires publics ou privés.



16th International Conference on Greenhouse Gas Control Technologies, GHGT-16

23rd -27th October 2022, Lyon, France

Quantitative monitoring of dissolved gases in a flooded borehole: calibration of the analytical tools

Van-Hoan Le^{a,b}, Marie-Camille Caumon^{a*}, Jacques Pironon^a, Philippe de Donato^a,
Médéric Piedevache^c, Aurélien Randi^a, Catherine Lorgeoux^a, Odile Barres^a

^aUniversité de Lorraine, CNRS, GeoRessources laboratory, F-54506 Vandœuvre-lès-Nancy, France

^bUniversity Grenoble Alpes, CEA, LETI, Grenoble, France

^cSolexperts France, 10 allée de la Forêt de la Reine, 54500 Vandœuvre-lès-Nancy, France

Abstract

Gas monitoring is a prerequisite to understand the exchange, diffusion, and migration processes of natural gases within underground environments, which is involved in several applications such as geological sequestration of CO₂. In this study, three different techniques (micro-GC, infrared and Raman spectroscopies) were deployed on an experimental flooded borehole for a monitoring purpose after CO₂ injection. The aim was to develop a real-time chemical monitoring device to follow gas concentrations in water by measurements in water inside the borehole but also at surface through a gas collection system in equilibrium with the borehole water. However, all three techniques must be calibrated to provide the most accurate quantitative data. For this, a first step of calibration in laboratory was carried out. New calibrations were required to determine partial pressure and/or concentrations of gases in water or in the gas collection system. For gas phase analysis, micro-GC, FTIR spectroscopy and Raman spectroscopy were compared. New calibration of the micro-GC was done for CO₂, CH₄ and N₂ with uncertainty from ± 100 ppm to 1.5 mol% depending on the bulk concentration and the type of gas. The FTIR and Raman spectrometers were previously calibrated for CO₂, and CO₂, N₂, O₂, CH₄, H₂O, respectively with an accuracy of 1%-6% depending on concentration scale, gas and spectrometer. Dissolved CO₂ in water was measured using a Raman spectrometer equipped with an immersion probe. The uncertainty on the predicted dissolved CO₂ concentration and partial pressure was of ± 0.003 mol.kg⁻¹ and ± 0.05 bar, respectively.

Keywords: chemical monitoring, multi-sensors, CO₂ injection, dissolved gas, calibration

1. Introduction

Since the last decades, the research projects relating to the monitoring of the underground gas content within a borehole are still a topical subject that is directly involved in several environmental preservation applications. For instance, face to global warming and climate change, numerous carbon capture, utilization and storage projects (CCUS) are performed around the world [1, 2] to reduce the anthropogenic greenhouse gas emission into the atmosphere such as the Century Plant CCUS project in the USA, the Sleipner CCUS project in Norway [3], the Shenhua CCUS project in China [4], and the Lacq-Rousse CCS project in France [5, 6], etc. Within such application, the monitoring strategy of the soil gas content variation must be deployed before CO₂ injection (to establish the

* Corresponding author. Tel.: +33 3 72 74 55 37, E-mail address: marie-camille.caumon@univ-lorraine.fr

baseline concentration variation and to define the alert limitation) and during and after CO₂ injection (to detect as soon as possible any CO₂ leakage and environmental impacts). The geological sequestration of the nuclear waste also received huge attention from the scientific community with many studies in which the confining properties of the host rock of the geological storage site were investigated to assess its long-term safety [7–10]. For that, the evolution of the concentration of dissolved gases (CO₂, CO, CH₄, C₂H₆, C₃H₈, N₂, H₂, O₂, H₂S, etc.) of the pore water is the key information to understand the fluid-rock interaction mechanisms and the transport properties of solutes within the host rock [8, 10].

Intense efforts have been made on the metrological development including the optimization of the experimental protocol and the data processing or the enhancement of the accuracy of the measurement [8, 11–14]. Since the chemical composition of the (dissolved) gases within the underground medium is not fully known in prior, the combination of different techniques is envisaged in order to detect and quantify in-situ and continuously as much gas as possible. Nowadays, the Fourier transform infrared (FTIR) and the Raman vibrational spectroscopies are widely used for continuous measurement of natural gas analyses [15, 16, 14, 17, 18]. The quantitative measurement using vibrational spectroscopy is not straightforward analysis but requires first precise calibration of the signal of each gas with respect to the properties of interest (e.g., molar proportion, partial pressure). Since the signal from vibrational spectroscopy is particularly sensitive to different instrumental parameters (excitation wavelength, response function of the device) as well as the operational environmental conditions (pressure, temperature), the calibration is therefore device-specific and should be regularly re-calibrated to ensure the highest accuracy of measurement. It is to note that FTIR spectroscopy presents some intrinsic limitations. For instance, the spectra of the combination band of CO₂ (centered at 3610 cm⁻¹) are strongly affected by the H₂O vapor contribution at some concentration ranges and required a specific additional processing [16]. Also, the homonuclear diatomic gases (such as N₂, O₂) cannot be detected by FTIR spectroscopy whereas they are an important indicator about the biological activity of the soil (e.g., soil respiration processes) and the oxygenation conditions [19, 17, 20–22]. On the other hand, the Raman technique can detect the most common natural gases (including CO₂, CH₄ as well as H₂, O₂ and N₂...) but with lower sensitivity compared to that of FTIR spectroscopy. Combining these two techniques can thus bring interesting and complementary information to each other. Besides, the micro gas chromatograph (micro-GC), which is a molecular separative technique, is a powerful technique with very high sensitivity and reproducibility for natural gas analyses. Using at least two modules with two different column and carrier gas, all the pre-cited gases can be analyzed.

The *in-situ* and continuous measurement of the dissolved gas concentration within an aquifer or the aqueous phase of the borehole is still challenging due to the technical limitation of the instruments (e.g., low sensitivity of the Raman spectroscopy, the lack of accurate calibration data). Assuming that the partial pressures of the gases dissolved within the liquid and the gaseous phases above the liquid are in equilibrium [23], the dissolved gas concentration within an aquifer or a flooded borehole can be thus indirectly measured by analyzing its gaseous form. For this purpose, the specific membrane-based completion SysMoG designed by Solexperts was developed which permitted the collection of dissolved gas but excluded water [5]. The collected dissolved gases can thereby be transported from the aquifer or the flooded depth borehole via a gas circulation system to different analytical techniques to be analyzed. Besides, the dissolved concentration or the partial pressure of CO₂ can also be derived from the pore water *ex-situ* analysis, e.g., calculated from the measured alkalinity or the total inorganic carbon content using PHREEQC software [8, 24]. However, the pore water extraction requires a careful sampling procedure to avoid any sample chemical alteration (due to the contact with the atmosphere for example) which in turn may result in an error of the measured dissolved gas concentration. Indeed, there was a noticeable discrepancy between the partial pressure or the concentration of dissolved CO₂ measured from the gaseous phase and from water composition which could not be fully interpreted [8]. Thus, more experiments are still needed to investigate the gas membrane transfers to better interpret the evolution of the dissolved gas concentration. For this purpose, an experimental borehole of 51-meter depth drilled by Solexperts is devoted to develop and test the experimental protocol and new analytical instruments before deploying them in the field. The borehole is equipped with a specific membrane-based completion SysMoG and a closed gas circulation system which allows continuous gas analysis by different techniques. Several CO₂ injections into water within the borehole were performed to simulate a CO₂ leakage. The micro-GC, Raman and FTIR spectroscopies are connected all together to the gas circulation system to do the *in-situ* analysis.

The purpose of this study is to calibrate and compare the performance of the instruments in quantifying dissolved gases before using them on-line with the instrumented borehole. Here the calibration procedure and the new calibration

data for the quantitative analysis of CO₂, CH₄ and N₂ concentrations are detailed. The application of these calibrations to the measurement in the borehole during CO₂ injection will be published in a dedicated paper [25].

2. Material and methods

2.1. Description of the experimental borehole

The experimental site consists of a borehole of 51-meter depth and 10 cm diameter, drilled by Solexperts (Vandœuvre-lès-Nancy, France). The borehole is entirely isolated from its surrounding medium, i.e., there is no contact between the borehole and the adjacent soil or the groundwater. The piezometer level within the borehole is freely adjusted by adding or removing water. The hydrostatic pressure at the bottom of the borehole is ~ 3-5 bars and temperature ~ 10 °C. For the *in-situ* continuous measurement of the gas concentration, a SysMoG completion specifically designed by Solexperts is installed into the borehole and connected to the analytical instruments placed at the ground via a gas circulation system.

The gases dissolved in the aqueous phase equilibrate across the hydrophobic membrane into a gas collection chamber (GCC). A gas circulation line connects the GCC of the completion to the analytical module placed at the ground in a closed system. The analytical instruments are set up at the ground including a FTIR spectrometer, a micro gas chromatograph (micro-GC), and two Raman spectrometers for continuous monitoring of the concentration of the different gases (e.g., CO₂, CH₄, N₂, O₂, H₂O). One Raman spectrometer is equipped with an immersion probe to directly measure gas concentration dissolved in water inside the borehole. The other instruments, i.e. FTIR, micro-GC and the second Raman spectrometer, are used to analyze the gases from the gas collection chamber.

2.2. Laboratory experimental setup to determine dissolved CO₂ concentration by Raman spectroscopy

The signal of the Raman RNX2 spectrometer (Kaiser Optical Systems) coupled with an immersion probe (WetHeadTM) is calibrated to determine the concentration of CO₂ dissolved in water. It is done by acquiring the Raman spectra of a water solution equilibrated with a known pressure of CO₂ at known temperature. Indeed, according to Henry's law [23] the concentration of a gas dissolved in a solution at equilibrium is proportional to its partial pressure within the vapor phase, which is above the liquid phase, and can be calculated by equation (1):

$$C_{CO_2} = K_H^\circ \cdot p \quad (1)$$

where C_{CO_2} is the concentration of the dissolved CO₂ (mol·kg⁻¹), p is the partial pressure of CO₂ in a gaseous phase, K_H° is Henry's law constant for the solubility of CO₂ at 298.15K, (i.e., $K_H^\circ = 0.034$ mol·kg⁻¹·bar⁻¹) [26]. The Henry's law constant at a given temperature T (K_H^T) can be calculated from K_H° using equation (2):

$$K_H^T = K_H^\circ \cdot \exp\left(2400 \cdot \left(\frac{1}{K} - \frac{1}{298.15}\right)\right) \quad (2)$$

The Raman spectra of CO₂ dissolved in water at different equilibrium states are recorded by using the experimental setup shown in Fig. 1. The calibration apparatus consists of a 1000-mL airtight stainless-steel cylinder (Swagelok, Fig. 1.1) in where water is equilibrated with CO₂ at controlled pressures. One end of the cylinder is connected to a pump (Fig. 1.2), a pressure transducer (Fig. 1.3), and a bottle of CO₂ via a union cross (Swagelok) (Fig. 1.4). Three valves are firstly closed and the cylinder is then inversed and fill with about 500 ml of water into the cylinder via its bottom end (Fig. 1.5). The immersion probe is then inserted into the cylinder in a way to ensure that the head of the immersion probe is still under the water level when the cylinder is closed and inversed again (Fig. 1.6). The cylinder is closed by a specific tor ensuring there is no gas or water leakage and then vertically fixed with a stand. The Raman probe is connected to a Raman RXN2 spectrometer (Fig. 1.7) by a 100-m long optical fiber. Before introducing CO₂

into the cylinder, the entire system is evacuated under vacuum to remove the air inside the cylinder. Once the purge is done, CO₂ is introduced into the cylinder at the desired pressure via the gas inlet (Fig. 1.4) by using a pressure regulator connected to the compressed CO₂ bottle (99.99% purity, Air Liquid). The internal pressure is monitored by the pressure transducer (Fig. 1.3). Room temperature is also monitored. Thus CO₂ gradually dissolves into water at controlled conditions (P and T).

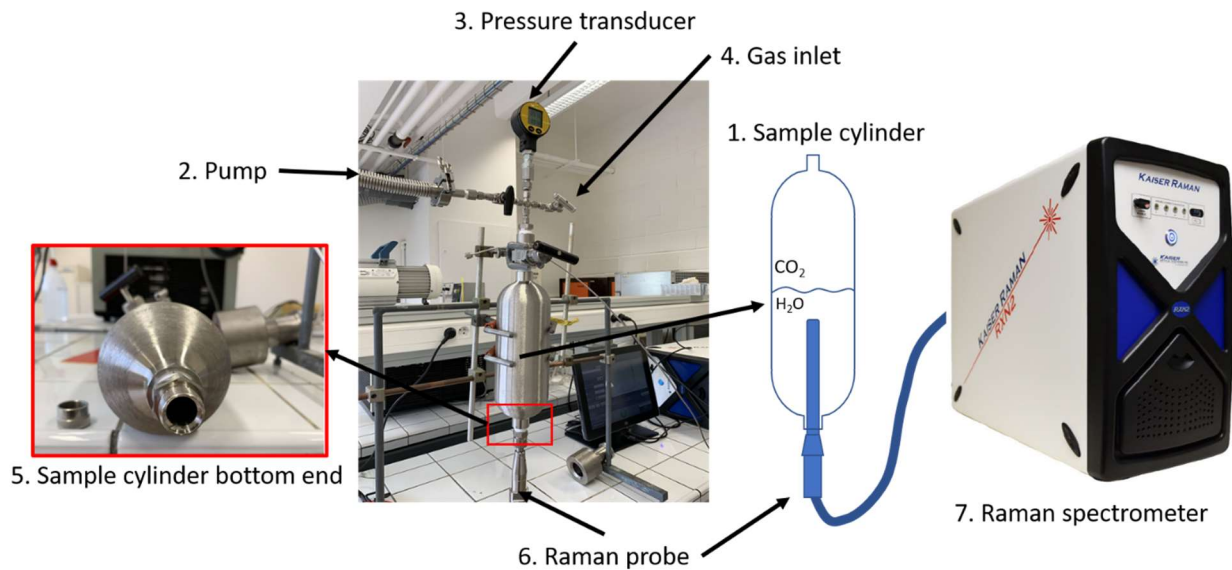


Fig. 1: Experimental setup to measure the Raman signal of dissolved CO₂ as a function of pressure. (1) 1000-mL stainless-steel cylinder. The upper end of the cylinder is connected to a pump (2), a pressure transducer (3) and a bottle of pure compressed CO₂ (4). The Raman probe (6) is introduced via the other end of the cylinder which is then closed by a special tor to ensure there is no water leakage. The Raman probe is connected to a Raman RXN2 spectrometer (7) by a 100-m optical fiber.

CO₂ and H₂O Raman spectra are simultaneously recorded over the spectral range 1350-1850 cm⁻¹ with the Raman RXN2 spectrometer. The wavelength and power of the excitation radiation are 532 nm and ~ 100 mW, respectively. The acquisition time is 30 seconds per accumulation, and 3 accumulations for each measurement. An example of spectra of CO₂ dissolved in water is shown in Fig. 2. The obtained spectra were then processed by LabSpec6 software (Horiba) to determine the peak area of CO₂ and H₂O after baseline subtraction. As the area of the lower band of CO₂ at ~ 1285 cm⁻¹ is too small, only the area of the upper band of CO₂ at ~ 1381 cm⁻¹ was considered. Besides, the Raman H-O-H bending mode of water is observed over a spectral range from 1450-1800 cm⁻¹ which superimposes the signal of the sapphire windows of the immersion probe at ~ 1522 cm⁻¹ (Fig. 2). Thus, the total peak area of the H₂O band was calculated after subtracting the signal of sapphire.

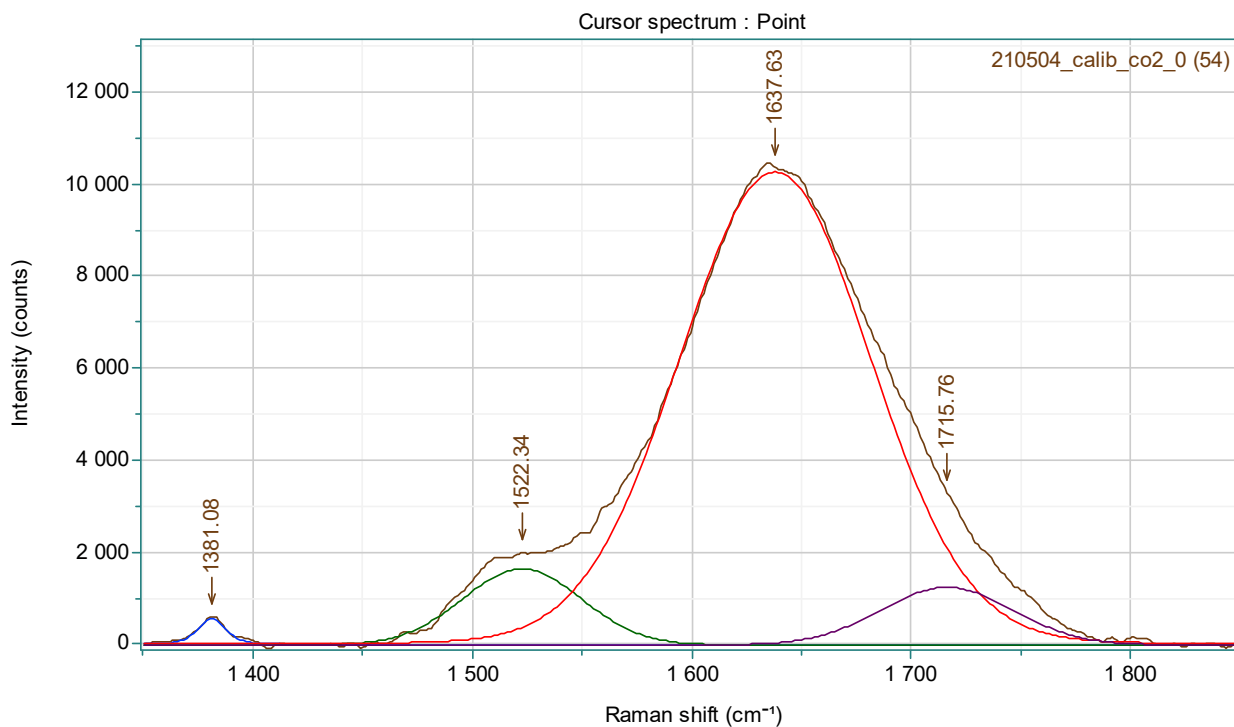


Fig. 2: Raman spectra of CO₂ dissolved in water under a pressure of 0.75 bar after baseline subtraction. The upper band of the CO₂ Fermi diad is observed at 1381 cm⁻¹. The H–O–H bending mode of H₂O is observed in the range 1450-1800 cm⁻¹.

The internal pressure of the tanker was firstly set at ~ 2 bars. The time needed to reach the equilibrium is more than 3 days (Fig. 5). When pressure increases from 2 bars (at equilibrium) to 3 bars, the time needed to reach the new equilibrium state at 3 bars is less than one day. Afterward, the pressure is successively decreased to ~ 2.5, 1.5, 1, 0.7, 0.5, 0.3, and 0.1 bar by adjusting the pressure regulator of the gas bottle and/or opening the valve v1. The equilibrium state at these lower pressures is reached after few hours. Shaking of the entire tanker can help to speed up the equilibrium process.

2.3. Determination of the concentrations in the gas phase

2.3.1. Micro-GC calibration

The micro-GC-490 (Agilent) was calibrated for the quantitative measurement of CO₂, CH₄ and N₂. CH₄ and N₂ were quantified using a module with a Molsieve 5Å column (10 m) with argon as carrier gas and CO₂ using the module with a PoraplotU column (10 m) with helium as carrier gas. For the two modules, injection time is 50 ms, injector temperature is 90 °C, carrier gas pressure is 30 psi and detectors are micro catarometer (μTCD). The column temperature is 145 °C for the Molsieve module and 80°C for the PoraplotU module. Peak integration is done with Soprane Software (SRA). Calibrations were established using reference gases of known concentration (commercial standard gases with certified concentration, the uncertainty is less than 1%) or gas mixtures prepared in the laboratory from pure gases by using a gas mixer (GasMix™-AlyTech). The uncertainty on the concentration of the prepared gas mixtures is less than 3%. To ensure the highest accuracy of the calibration data at a low concentration range, the concentration of some prepared gas mixtures whose the concentration is less than 4000 ppm is re-checked by G2201-i analyzer (Picarro, Inc.).

Upon the calibration procedure, the entrance of the micro-GC is directly connected to the bottle of standard gas or the outlet of the AlyTech gas mixer (Fig. 3). To introduce the gases into the micro-GC, an external pump is used and turn on for about 20 seconds to remove any atmospheric air in the system. Once this is done, the reference gases are

introduced at a pressure less than 1.5 bar. Thereby, the whole volume of the external pump and connecting tubes is filled only by the reference gas. The reference gas is then injected into the analysis modules to be analyzed thanks to the internal pump (Fig. 3).

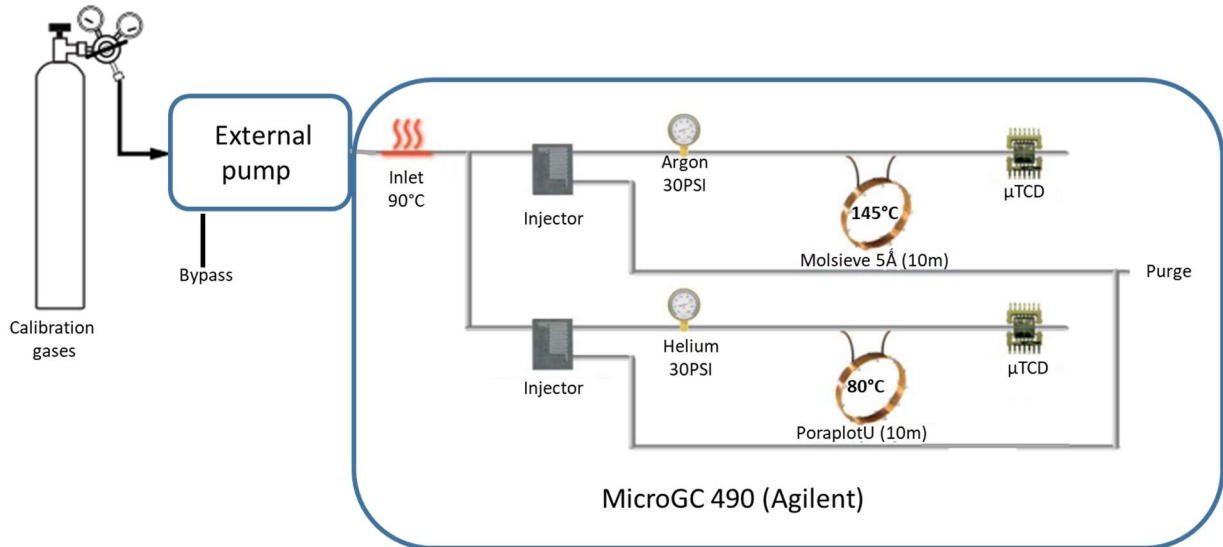


Fig. 3: Simplified scheme describing the gas circulation within the micro-GC 490.

2.3.2. FTIR spectrometer calibration

The IR measurements are performed using a portable FTIR Bruker Alpha spectrometer (Bruker Optics GmbH, Germany) equipped with a 5 cm path-length stainless-steel gas cell. The latter is equipped with two ZnSe (Zinc Selenide) windows and directly connected to the gas circuit for continuous measurement of gas concentration. The IR spectra are scanned 16 times over the spectral range 600 - 4000 cm^{-1} .

The calibration data of the FTIR apparatus used herein (including the spectrometer and the gas cell) for the quantification of CO_2 concentration over a range from 100 to 60 000 ppm was established in a previous work [22] (Fig. 4). As shown in Fig. 4, the calibration curve links the CO_2 concentration (ppm) to the variation of the peak area of the fundamental band ν_3 of CO_2 at $\sim 2350 \text{ cm}^{-1}$. According to the authors, the accuracy of the CO_2 concentration measurement is less than 6% at < 2000 ppm, less than 4% at under 5000 ppm, less than 2% at under 30 000 ppm, and less than 1% at under 100 000 ppm.

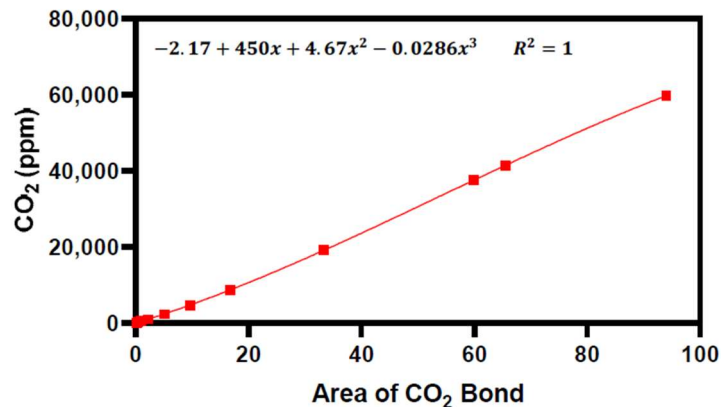


Fig. 4: Calibration curve linking the CO_2 concentration (from 200 to 60 000 ppm) to the area of the IR fundamental bands of CO_2 (at 2350 cm^{-1}) [22].

2.3.3. Raman spectrometer calibration

The molar fraction (X_i , mol%) of gaseous species within a mixture can be determined from the Raman scattering cross-section (σ_i) of the vibrational mode of gases and the corresponding peak area (A_i) by using equation (3) [27]:

$$X_i = \frac{\left(\frac{A_i}{\sigma_i \zeta_i}\right)}{\sum_1^i \left(\frac{A_i}{\sigma_i \zeta_i}\right)} \quad (3)$$

where ζ_i is the instrumental efficiency which depends on wavelength (peak position). As the spectrometer intensity response was calibrated using a reference emission lamp (HCA, Kaiser Optical System), all ζ_i was equal for all gases. Therefore, the σ_i values from literature of N₂, CO₂, CH₄, O₂ and H₂O for the excitation wavelength of 532 nm can be used [28, 29] (Table 1).

Table 1: Raman peak position and corresponding scattering cross-section (σ) for an excitation wavelength of 532 nm

	Peak position (cm ⁻¹)	σ
CO ₂ (upper band)	1388	1.54
CH ₄	2917	7.73
N ₂	2331	1
O ₂	1555	1.24
H ₂	4153	2.3
H ₂ O vapor	3665	2.35

The Raman measurements of the gases flowing within the gas circulation lines are performed using a Raman RXN1 spectrometer equipped with a 532 nm Nd-YAG excitation laser, and coupled with a gas probe (AirHead™, Kaiser Optical Systems, Inc.) via a 5-meter-long optical fiber. The air probe is embedded by a dedicatedly designed stainless steel gas cell equipped with a sapphire window and an array of mirrors to amplify the Raman scattering intensity that is connected to the gas circulation systems. The Raman analyses can be thereby continuously performed without changing the internal pressure and the composition of the collected gases. The peak area of the studied gases is measured by integrating their Raman spectrum over a predefined spectral interval, i.e., between 1380 cm⁻¹ and 1397 cm⁻¹ for the upper band of CO₂ (at 1388 cm⁻¹), between 2319 cm⁻¹ and 2341 cm⁻¹ for the N₂ band, between 1545 cm⁻¹ and 1566 cm⁻¹ for O₂, and from 3637 cm⁻¹ to 3665 cm⁻¹ for H₂O.

3. Calibration data for quantitative measurements

3.1. Quantifying dissolved CO₂ concentration by Raman spectroscopy

The evolution of the CO₂-to-H₂O peak area ratio (PAR) as a function of time is presented in Fig. 5. In general, the PAR increases gradually with time following the increase of the amount of dissolved CO₂ then becomes unchanged once the equilibrium state is reached. The average value of PAR at each equilibrium state and its standard deviation are reported in Table 2 with the corresponding concentration of CO₂.

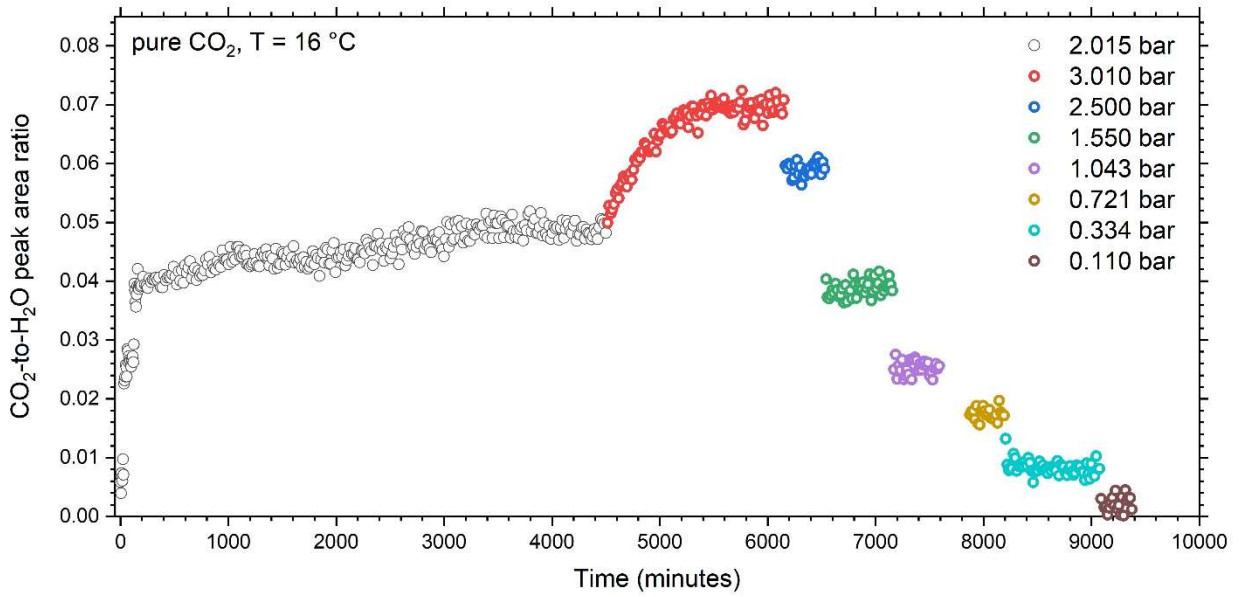


Fig. 5: Evolution of carbon dioxide-to-water peak area ratio (A_{CO_2}/A_{H_2O}) as a function of time (minutes) and pressure (bar).

Table 2: PAR as a function of pressure and CO₂ concentration

Partial pressure of CO ₂ (bar)	Dissolved CO ₂ concentration ^(a) (mol/kg)	Average peak area ratio ^(b) (A_{CO_2}/A_{H_2O})	Standard deviation
3.010	0.1315	0.06957	0.00120
2.500	0.1092	0.05905	0.00116
2.015	0.0880	0.04874	0.00139
1.550	0.0677	0.03872	0.00134
1.043	0.0456	0.02527	0.00121
0.721	0.0315	0.01740	0.00102
0.334	0.0146	0.00794	0.00094
0.115	0.0048	0.00218	0.00126

^(a) Calculated from pressure and temperature using Henry's law constant. ^(b) The average peak area ratio is calculated from all experimental data point at equilibrium (Fig. 5). The calibration curve is fitted from all experimental data points, linking the variation of the PAR to the concentration of the dissolved CO₂ (Fig. 6a) or the partial pressure of the CO₂ (Fig. 6b). The uncertainty (1σ) of the predicted CO₂ dissolved concentration and the partial pressure are $\pm 0.003 \text{ mol.kg}^{-1}$ and $\pm 0.05 \text{ bar}$, respectively.

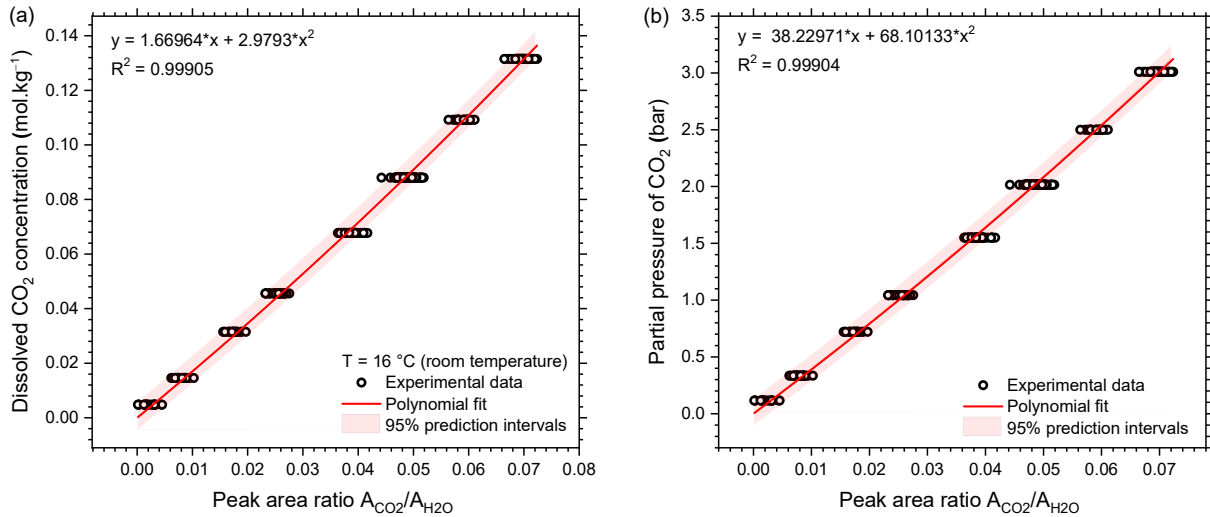


Fig. 6: Relationship between the peak area ratio A_{CO_2}/A_{H_2O} (PAR) and (a) the concentration of CO₂ dissolved in water or (b) CO₂ partial pressure.

The calibration curves are fitted from all experimental data points, linking the variation of the PAR to the concentration of the dissolved CO₂ (Fig. 6a) and the partial pressure of the CO₂ (Fig. 6b). The uncertainty (1σ) of the predicted dissolved CO₂ concentration and the partial pressure is about $\pm 0.003\text{ mol.kg}^{-1}$ and $\pm 0.05\text{ bar}$, respectively.

3.2. Gas concentration determined by Micro-GC

In general, the calibration curves of the micro-GC-490 are a linear correlation between the peak area and the concentration (ppm). The signal saturates when the CO₂ concentration is above 60 mol%. Consequently, in the present study, only two calibration curves of CO₂ are provided for low (from 500 to 9000 ppm) and intermediate concentration ranges (up to $\sim 60\%$) (Fig. 7). The uncertainty of the predicted CO₂ concentration (at 1σ , estimated from the prediction intervals of the regression equation) is less than $\pm 100\text{ ppm}$ for the concentration range under 9000 ppm, $< \pm 1000\text{ ppm}$ for the concentration range under 100 000 ppm, and $< \pm 0.5\%$ for the concentration range under 60 mol%.

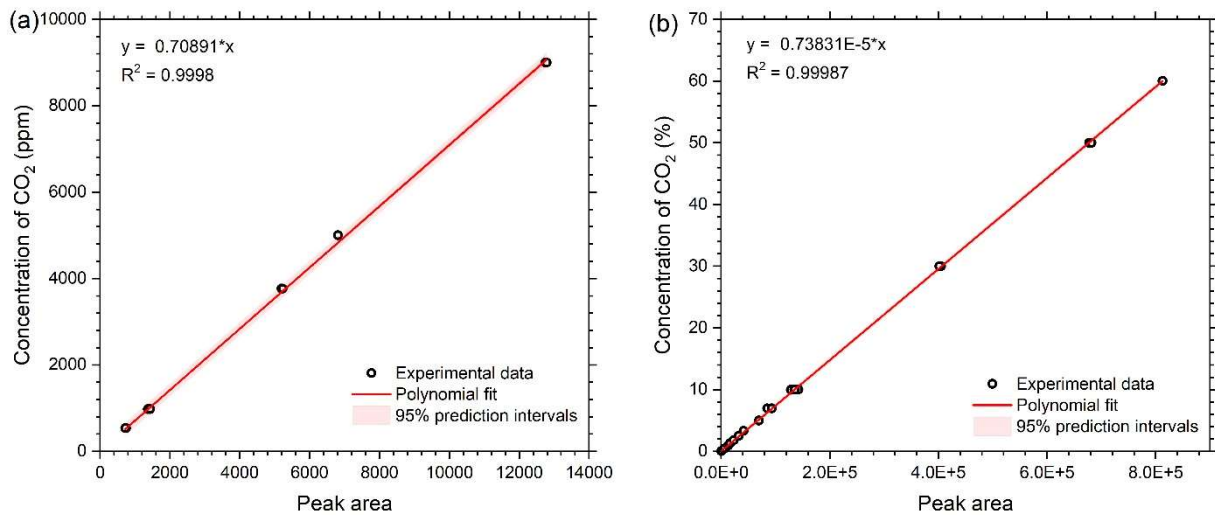


Fig. 7: Calibration of CO₂ signal for (a) low and (b) intermediate concentration range, i.e., $< 9000\text{ ppm}$ and $< 60\text{ mol}\%$, respectively.

In the same way calibration data was established over a concentration range from 0 to 5000 ppm for CH₄, and from 1-100% for N₂ (Fig. 8). The uncertainty of the predicted concentration of CH₄ and N₂ (1 σ , estimated from the prediction intervals) is less than about ± 100 ppm and 1.5 mol%, respectively.

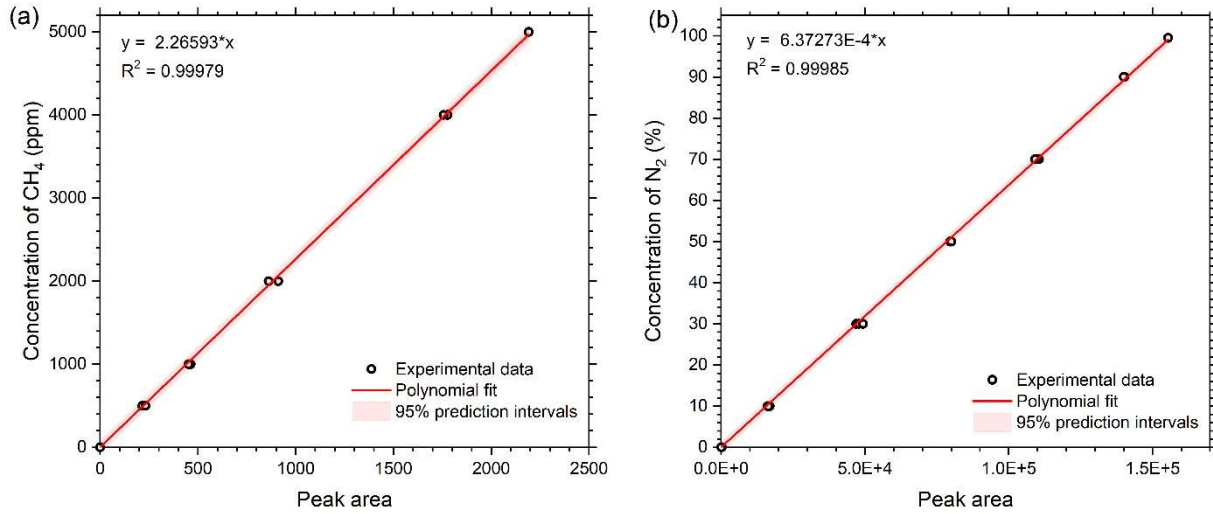


Fig. 8: Calibration data of (a) CH₄ for a concentration range from 0 to 5000 ppm or (b) N₂ for a concentration range from 0 to 100 mol%

3.3. Gaseous CO₂ concentration determined by FTIR

In the present study, the CO₂ concentration within the gaseous phase of the borehole is expected to range from about 500 ppm (near the atmospheric concentration) to 60 mol%. Since the intensity of the IR fundamental band of CO₂ at ~ 2350 cm⁻¹ is quickly saturated above 60 000 ppm, the peak area of the combination bands of CO₂ at ~ 3610 cm⁻¹ ($\nu_1 + \nu_3$ and $2\nu_2 + \nu_3$) is therefore used. It is to note that there is an interference between the IR spectra of the combination bands of CO₂ and that of H₂O vapor around 3610 cm⁻¹. The subtraction of the signal of H₂O vapor from that of CO₂ is thus required to ensure the highest accuracy of the concentration measurement. More details about FTIR data processing can be found in Taquet *et al.* [14]. Moreover, it is also to note that the existing calibration data of the FTIR Alpha spectrometer was usually established at atmospheric pressure, whereas the intensity and the area of the IR spectra vary as a function of pressure. In this study, the total pressure within the gas circulation system is however expected to vary from the atmospheric pressure to \sim up to 2-3 bars due to a large amount of CO₂ dissolved in the aqueous phase, then penetrating across the membrane into the GCC. The calibration data for such a wide pressure and concentration range is not available yet. In the borehole, the FTIR spectra are simultaneously recorded with Raman and micro-GC whose intensity does not depend on the total pressure. Therefore, new calibration curves linking the IR peak area of the combination band of CO₂ to the concentration measured by other techniques (Raman and micro-GC) are thereby established for the pressure and concentration range encountered in the borehole by comparison with Raman spectroscopy and GC [25].

3.4. Gas concentration determined by Raman spectroscopy

Partial pressure and mol% in the gas mixture are determined by Raman spectroscopy using literature data (Table 1) and pressure measurement. Previous works using the same Raman spectrometer and the same probe reported uncertainties of about 0.5-1 mol% at atmospheric pressure [14, 18]. The detection limit depends on the cross section of each gas: the best detection limit is for CH₄ and the lowest one for N₂ (Table 1) at about 0.002 mbar and 0.01 mbar, respectively.

4. Conclusion

In preparation of on-site measurement of gas concentration in a flooded borehole, laboratory calibrations are carried out for micro-GC, FTIR spectroscopy and Raman spectroscopy. Raman spectroscopy is the only of the three techniques able to quantitatively measure the concentration of CO₂ dissolved in water, with an accuracy of 0.003 mol.kg⁻¹ or 0.05 bar for the corresponding partial pressure in equilibrium with the solution. For the gas phase, Raman spectroscopy can detect all the studied gases (CO₂, CH₄, N₂, O₂, H₂, H₂O) with an accuracy better than 1 mol% and a detection limit lower than 0.01 mbar. The Micro-GC is calibrated to quantify CO₂, CH₄ and N₂ with quite much lower detection limit (< 100 ppm) and higher accuracy (100 ppm – 5% depending on the concentration range). Finally, FTIR can quantify CO₂ concentration in the gas phase over the full concentration range (500 ppm -100%) with an accuracy depending on the concentration range (1% - 6%). At concentration higher than 60 mol% and pressure higher than atmospheric pressure, the infrared spectrometer is not yet calibrated. Next acquisition in the flooded borehole will lead to a new calibration in this high-level range by comparison with micro-GC and Raman spectroscopy data [25]. The performance and applicability of each technique and of the polymeric membrane responsivity and resistance over a wide concentration-pressure range will be evaluated and compared during the measurement run on the instrumented borehole.

Acknowledgements

The authors would like to thank the GEODERNEGIES (Scientific Interest Group), for its financial support through the OUROBOROS (2019-2021) research program.

References

- [1] Bui, M.; Adjiman, C.S.; Bardow, A.; Anthony, E.J.; Boston, A.; Brown, S.; Fennell, P.S.; Fuss, S.; Galindo, A.; Hackett, L.A.; Hallett, J.P.; Herzog, H.J.; Jackson, G.; Kemper, J.; Krevor, S.; Maitland, G.C.; Matuszewski, M.; Metcalfe, I.S.; Petit, C.; Puxty, G.; Reimer, J.; Reiner, D.M.; Rubin, E.S.; Scott, S.A.; Shah, N.; Smit, B.; Trusler, J.P.M.; Webley, P.; Wilcox, J. and Dowell, N.M.: Carbon capture and storage (CCS): the way forward, *Energy & Environmental Science*, **11** (2018), no. 5, pp. 1062–1176.
- [2] Li, H.; Jiang, H.-D.; Yang, B. and Liao, H.: An analysis of research hotspots and modeling techniques on carbon capture and storage, *Science of The Total Environment*, **687** (2019), pp. 687–701.
- [3] Solomon, S.: Carbon Dioxide Storage: Geological Security and Environmental Issues—Case Study on the Sleipner Gas Field in Norway. The Bellona Foundation, Oslo, Norway, (2006).
- [4] Li, Q.; Liu, G.; Liu, X. and Li, X.: Application of a health, safety, and environmental screening and ranking framework to the Shenhua CCS project, *International Journal of Greenhouse Gas Control*, **17** (2013), pp. 504–514.
- [5] Taquet, N.: Monitoring Geochimique de la geosphère et de l’atmosphère : application au stockage géologique du CO₂2012.
- [6] Monne, J. and Prinnet, C.: Lacq-Rousse Industrial CCS Reference Project: Description and Operational Feedback after two and Half Years of Operation, *Energy Procedia*, **37** (2013), pp. 6444–6457.
- [7] Rübel, A.P.; Sonntag, C.; Lippmann, J.; Pearson, F.J. and Gautschi, A.: Solute transport in formations of very low permeability: profiles of stable isotope and dissolved noble gas contents of pore water in the Opalinus Clay, Mont Terri, Switzerland, *Geochimica et Cosmochimica Acta*, **66** (2002), no. 8, pp. 1311–1321.
- [8] Vinsot, A.; Appelo, C.A.J.; Cailteau, C.; Wechner, S.; Pironon, J.; De Donato, P.; De Cannière, P.; Mettler, S.; Wersin, P. and Gäbler, H.-E.: CO₂ data on gas and pore water sampled in situ in the Opalinus Clay at the Mont Terri rock laboratory, *Physics and Chemistry of the Earth, Parts A/B/C*, **33** (2008), pp. S54–S60.
- [9] Gaucher, E.C.; Tournassat, C.; Pearson, F.J.; Blanc, P.; Crouzet, C.; Lerouge, C. and Altmann, S.: A robust model for pore-water chemistry of clayrock, *Geochimica et Cosmochimica Acta*, **73** (2009), no. 21, pp. 6470–6487.
- [10] Bossart, P.; Bernier, F.; Birkholzer, J.; Bruggeman, C.; Connolly, P.; Dewonck, S.; Fukaya, M.; Herfort, M.; Jensen, M.; Matray, J.-M.; Mayor, J.C.; Moeri, A.; Oyama, T.; Schuster, K.; Shigeta, N.; Vietor, T. and Wiczorek, K.: Mont Terri rock laboratory, 20 years of research: introduction, site characteristics and overview of experiments, *Swiss Journal of Geosciences*, **110** (2017), no. 1, pp. 3–22.
- [11] Laier, T. and Øbro, H.: Environmental and safety monitoring of the natural gas underground storage at Stenlille, Denmark, *Geological Society, London, Special Publications*, **313** (2009), no. 1, pp. 81–92.
- [12] Donato, P. de; Pironon, J.; Mouronval, G.; Hy-Billiot, J.; Garcia, B.; Lucas, H.; Pokryszka, Z.; Lafortune, S.; Flamant, P.H.; Cellier, P.; Gal, F.; Pierres, K.M.-L.; Pierres, K.L.; Taquet, N. and Barres, O.: SENTINELLE. Development of combined geochemical monitoring on Lacq pilot site from geosphere to atmosphere, conference ‘10. International Conference on Greenhouse Gas Control Technologies (GHGT 10)’, 2010.
- [13] Cailteau, C.; Pironon, J.; Donato, P. de; Vinsot, A.; Fierz, T.; Garnier, C. and Barres, O.: FT-IR metrology aspects for on-line monitoring of CO₂ and CH₄ in underground laboratory conditions, *Analytical Methods*, **3** (2011), no. 4, pp. 877–887.
- [14] Taquet, N.; Pironon, J.; De Donato, P.; Lucas, H. and Barres, O.: Efficiency of combined FTIR and Raman spectrometry for online quantification of soil gases: Application to the monitoring of carbon dioxide storage sites, *International Journal of Greenhouse Gas*

- Control, **12** (2013), pp. 359–371.
- [15] Dubessy, J.; Poty, B. and Ramboz, C.: Advances in C-O-H-N-S fluid geochemistry based on micro-Raman spectrometric analysis of fluid inclusions, *European Journal of Mineralogy*, (1989), pp. 517–534.
- [16] Cailteau, C.; Donato, P. de; Pironon, J.; Vinsot, A.; Garnier, C. and Barres, O.: In situ gas monitoring in clay rocks: mathematical developments for CO₂ and CH₄ partial pressure determination under non-controlled pressure conditions using FT-IR spectrometry, *Analytical Methods*, **3** (2011), no. 4, pp. 888–895.
- [17] Gal, F.; Michel, K.; Pokryszka, Z.; Lafortune, S.; Garcia, B.; Rouchon, V.; de Donato, P.; Pironon, J.; Barres, O.; Taquet, N.; Radilla, G.; Prinet, C.; Hy-Billiot, J.; Lescanne, M.; Cellier, P.; Lucas, H. and Gibert, F.: Study of the environmental variability of gaseous emanations over a CO₂ injection pilot—Application to the French Pyrenean foreland, *International Journal of Greenhouse Gas Control*, **21** (2014), pp. 177–190.
- [18] Lacroix, E.; Donato, P. de; Lafortune, S.; Caumon, M.-C.; Barres, O.; Liu, X.; Derrien, M. and Piedevache, M.: In situ continuous monitoring of dissolved gases (N₂, O₂, CO₂, H₂) prior to H₂ injection in an aquifer (Catenoy, France) by on-site Raman and infrared spectroscopies: instrumental assessment and geochemical baseline establishment, *Analytical Methods*, (2021).
- [19] Lloyd, J. and Taylor, J.A.: On the Temperature Dependence of Soil Respiration, *Functional Ecology*, **8** (1994), no. 3, pp. 315–323.
- [20] Angert, A.; Yakir, D.; Rodeghiero, M.; Preisler, Y.; Davidson, E.A. and Weiner, T.: Using O₂ to study the relationships between soil CO₂ efflux and soil respiration, *Biogeosciences*, **12** (2015), no. 7, pp. 2089–2099.
- [21] Barba, J.; Cueva, A.; Bahn, M.; Barron-Gafford, G.A.; Bond-Lamberty, B.; Hanson, P.J.; Jaimés, A.; Kulmala, L.; Pumpanen, J.; Scott, R.L.; Wohlfahrt, G. and Vargas, R.: Comparing ecosystem and soil respiration: Review and key challenges of tower-based and soil measurements, *Agricultural and Forest Meteorology*, **249** (2018), pp. 434–443.
- [22] Adisaputro, D.; De Donato, P.; Saint-Andre, L.; Barres, O.; Galy, C.; Nourrisson, G.; Piedevache, M. and Derrien, M.: Baseline Subsoil CO₂ Gas Measurements and Micrometeorological Monitoring: Above Canopy Turbulence Effects on the Subsoil CO₂ Dynamics in Temperate Deciduous Forest, *Applied Sciences*, **11** (2021), no. 4, p. 1753.
- [23] Henry, W. and Banks, J.: III. Experiments on the quantity of gases absorbed by water, at different temperatures, and under different pressures, *Philosophical Transactions of the Royal Society of London*, **93** (1803), pp. 29–274.
- [24] Vinsot, A.; Appelo, C.A.J.; Lundy, M.; Wechner, S.; Cailteau-Fischbach, C.; de Donato, P.; Pironon, J.; Lettry, Y.; Lerouge, C. and De Cannière, P.: Natural gas extraction and artificial gas injection experiments in Opalinus Clay, Mont Terri rock laboratory (Switzerland), *Swiss Journal of Geosciences*, **110** (2017), no. 1, pp. 375–390.
- [25] Le, V.-H.; Pironon, J.; De Donato, P.; Piedevache, M.; Randi, A.; Lorgeoux, C.; Caumon, M.-C. and Barres, O.: In-situ monitoring of dissolved gases within flooded borehole by multiples techniques (Raman, FTIR, micro-GC). Assessing of the gas membrane transfer equilibrium, (in prep.).
- [26] Mackay, D. and Shiu, W.Y.: A critical review of Henry's law constants for chemicals of environmental interest, *Journal of Physical and Chemical Reference Data*, **10** (1981), no. 4, pp. 1175–1199.
- [27] Pasteris, J.D.; Wopenka, B. and Seitz, J.C.: Practical aspects of quantitative laser Raman microprobe spectroscopy for the study of fluid inclusions, *Geochimica et Cosmochimica Acta*, **52** (1988), no. 5, pp. 979–988.
- [28] Schrötter, H.W. and Klöckner: Raman Scattering Cross Section in Gases and Liquids, *Topics in Current Physics*, 1979, pp. 123–164.
- [29] Burke, E.A.J.: Raman microspectrometry of fluid inclusions, *Lithos*, **55** (2001), no. 1, pp. 139–158.